

## MIT Open Access Articles

*Electrochemical Properties of Monoclinic NaNiO<sub>2</sub>*

The MIT Faculty has made this article openly available. **Please share** how this access benefits you. Your story matters.

**Citation:** Vassilaras, P., X. Ma, X. Li, and G. Ceder. Electrochemical Properties of Monoclinic NaNiO<sub>2</sub>. Journal of the Electrochemical Society 160, no. 2 (November 28, 2012): A207-A211. © 2012 The Electrochemical Society.

**As Published:** <http://dx.doi.org/10.1149/2.023302jes>

**Publisher:** Electrochemical Society

**Persistent URL:** <http://hdl.handle.net/1721.1/82533>

**Version:** Final published version: final published article, as it appeared in a journal, conference proceedings, or other formally published context

**Terms of Use:** Article is made available in accordance with the publisher's policy and may be subject to US copyright law. Please refer to the publisher's site for terms of use.





## Electrochemical Properties of Monoclinic $\text{NaNiO}_2$

Plousia Vassilaras, Xiaohua Ma, Xin Li, and Gerbrand Ceder<sup>\*,z</sup>

Department of Materials Science and Engineering, Massachusetts Institute of Technology, Cambridge, Massachusetts 02139, USA

Monoclinic  $\text{NaNiO}_2$  is re-investigated as a positive electrode material for sodium ion batteries. We observe reversible Na extraction and insertion of about 120 mAh/g when  $\text{NaNiO}_2$  is cycled between 1.25 V and 3.75 V, though discharge only proceeds to  $\text{Na}_{0.91}\text{NiO}_2$ . The voltage profile shows large and pronounced steps, which are fully reversible. Charging to 4.5 V leads to higher charge and discharge capacity, though with poor coulombic efficiency and rapid capacity fade. X-ray diffraction of charged samples indicates that high voltage charging leads to the formation of an inactive phase.

© 2012 The Electrochemical Society. [DOI: 10.1149/2.023302jes] All rights reserved.

Manuscript submitted June 13, 2012; revised manuscript received November 7, 2012. Published November 29, 2012.

$\text{Li}_x\text{MO}_2$  ( $M$  = transition metal) compounds have attracted wide attention because of their application as cathode materials for practical lithium ion batteries. Materials based on  $\text{LiCoO}_2$  and  $\text{LiNiO}_2$  are well studied as Li-intercalation materials, but others ( $M$  = V, Cr, Fe, Mn) do not reversibly de-intercalate lithium or do not easily form a layered structure ( $M$  = Ti, Fe, Mn).<sup>1–3</sup> On the other hand, one can find a limited number of reports on sodium de-intercalation from layered  $\text{NaMO}_2$  compounds ( $M$  = Ti, V, Cr, Mn, Fe, Co, Ni).<sup>2,4–12</sup> The Na compounds have a stronger tendency to form in the layered structure compared to  $\text{LiMO}_2$  because of the larger ionic radius difference between sodium and the transition metal.<sup>13,14</sup> Na compounds with mixed transition metals and either tunnel or layered structures, such as  $\text{Na}_x\text{Ni}_{0.6}\text{Co}_{0.4}\text{O}_2$ ,  $\text{Na}_x\text{Ni}_y\text{Mn}_{1-y}\text{O}_2$ ,  $\text{Na}_x\text{Ti}_y\text{Mn}_{1-y}\text{O}_2$ ,  $\text{NaNi}_{1/3}\text{Mn}_{1/3}\text{Co}_{1/3}\text{O}_2$ ,  $\text{Na}_x\text{Fe}_{0.5}\text{Mn}_{0.5}\text{O}_2$ , and  $\text{NaNi}_{1/3}\text{Fe}_{1/3}\text{Mn}_{1/3}\text{O}_2$  have also been studied as cathode materials.<sup>15–23</sup> While the layered structure consist of sheets of edge-shared  $\text{MO}_6$  octahedra, the tunnel structures consist of columns of edge-shared  $\text{MO}_5$  square pyramids and sheets of edge-shared  $\text{MO}_6$  octahedra.<sup>18</sup> In this paper we focus on layered  $\text{NaNiO}_2$  as a possible Na-intercalation cathode and show that, unlike in previous studies, a large amount of alkali ions can be reversibly cycled from  $\text{NaNiO}_2$ .

The structure of  $\text{NaNiO}_2$  was determined first in 1954 by film methods using a precession camera,<sup>24</sup> then in 1977 by Rietveld methods applying X-ray and neutron scattering,<sup>25</sup> and later in 2000 and 2005 by neutron and X-ray diffraction respectively.<sup>26,27</sup>  $\text{NaNiO}_2$  is stable as two polymorphs: a low-temperature layered  $\text{O}_3$  structure with a monoclinic structural distortion, and a higher temperature rhombohedral phase. The low temperature phase contains a Ni-O layer formed by edge-sharing  $\text{NiO}_6$  octahedra, each elongated due to the Jahn-Teller distortion of the  $\text{Ni}^{3+}$  ion. The Na ions lie between the  $\text{NiO}_2$  slabs and exhibit a distorted octahedral coordination by oxygen atoms.<sup>24–27</sup> This low temperature form of  $\text{NaNiO}_2$  is isostructural to  $\text{NaMnO}_2$ .<sup>12,28,29</sup> At temperatures around 450 K, the symmetry reduction due to the static Jahn-Teller effect is overcome by thermal motion, and the phase turns into a rhombohedral form.<sup>24–27</sup> This high temperature form of  $\text{NaNiO}_2$  is isostructural with  $\alpha\text{-NaFeO}_2$  or  $\text{LiNiO}_2$ .<sup>10,24</sup>

Monoclinic  $\text{NaNiO}_2$  has been previously synthesized and electrochemically tested as a cathode material, the results of which indicate a step-like character of the charge and discharge curve as well as an initial open circuit voltage of 2.47 V.<sup>30</sup> Furthermore, only 0.2 Na could be extracted from  $\text{NaNiO}_2$  during the first cycle.<sup>5,30,31</sup> In this paper, we report the synthesis and electrochemical testing of monoclinic  $\text{NaNiO}_2$ . Our results show a similar step-like character as well as a 2.60 V open circuit voltage, but in contrast to previous studies, our results show 199 mAh/g charge capacity ( $\Delta x = 0.85$  in  $\text{Na}_x\text{NiO}_2$ ) and 147 mAh/g discharge capacity ( $\Delta x = 0.62$  in  $\text{Na}_x\text{NiO}_2$ ) between 2.0 – 4.5 V. Cycling at 1.25–3.75 V shows that 0.63 Na can be de-intercalated and 0.52 Na intercalated back reversibly (corresponding to 147 mAh/g charge capacity and 123 mAh/g discharge capacity).

We also demonstrate reasonable capacity retention, when cycled in a limited voltage range.

### Experimental

$\text{NaNiO}_2$  was synthesized by solid-state reaction. Excess amounts of  $\text{Na}_2\text{O}$  (80%  $\text{Na}_2\text{O}$ , 20%  $\text{Na}_2\text{O}_2$ , Sigma Aldrich) and NiO (99%, Alfa Aesar) were mixed and ball milled for 4 hours at 500 rpm rate, and the resulting material was collected in the glove box. About 0.5 g of powder was fired in a Ni boat at 650°C under  $\text{O}_2$  for 14 hours before it was quenched to room temperature and moved to a glove box filled with argon. The as obtained black powder is sensitive to humid air and careful handling is necessary.

X-ray diffraction (XRD) patterns were collected on a Rigaku Rotaflex equipped with Cr K $\alpha$  radiation in the  $2\theta$  range of 15–130°. All the samples were sealed with Kapton film to avoid air exposure. Profile matching of the powder diffraction data of the as-prepared  $\text{NaNiO}_2$  was performed with Highscore Plus using space group C2/m.

Electrochemical cells were configured with Na/1 M  $\text{NaPF}_6$  in EC:DMC = 1:1/ $\text{NaNiO}_2$ , Super P carbon black (Timcal, 15 wt%) as conductive agent, and polyethylenetetrafluoride (PTFE) (DuPont, 5 wt%) as binder. The 1 M  $\text{NaPF}_6$  in EC:DMC electrolyte was prepared by dissolving anhydrous  $\text{NaPF}_6$  (98%, Sigma Aldrich) into EC:DMC (anhydrous, Sigma Aldrich, 1:1 in volume ratio). Two pieces of glass fiber served as separators and stainless steel as current collectors in Swagelok cells, assembled in an argon-filled glove box with the moisture level and oxygen level less than 0.1 ppm. The loading density of the active material used was in the range of 2.4–3.6 mg/cm<sup>2</sup>. The cells were cycled at room temperature using a Solatron 1287 operating in either galvanostatic or cyclic voltammogram mode.

The Na content vs. voltage was measured by potentiostatic intermittent titration (PITT) on a Solatron 1287 electrochemical potentiostat. Steps of 10 mV were taken to fully charge and discharge the cell. The capacity was measured at each voltage step until the current was below C/50.

### Experimental Results

The as-prepared room temperature  $\text{NaNiO}_2$  has a layered structure with monoclinic, C2/m symmetry as shown on the XRD pattern in Figure 1. The background and three broad peaks between 10–30° are due to the Kapton film, which is used to seal the sample. Rietveld refinement gives the lattice parameters  $a = 5.322$  Å,  $b = 2.845$  Å,  $c = 5.584$  Å,  $\beta = 110.467^\circ$ , values which are in close approximation to the results of both Dick et al.,<sup>25</sup> Chappel, et. al.<sup>26</sup> and Sofin, et. al.<sup>27</sup> ( $a = 5.318$  Å,  $b = 2.846$  Å,  $c = 5.582$  Å,  $\beta = 110.409^\circ$ ). The Ni-O layer is formed by edge sharing of Jahn-Teller elongated  $\text{NiO}_6$  octahedra with Ni-O distances of 1.932 Å ( $4\times$ ) and 2.177 Å ( $2\times$ ), and the Na ions between these layers also exhibit a distorted octahedral coordination with Na-O distances of 2.300 Å ( $4\times$ ) and 2.330 Å ( $2\times$ ). Cell parameters and atomic positions are listed in Table I.

\*Electrochemical Society Active Member.

<sup>z</sup>E-mail: gceder@mit.edu

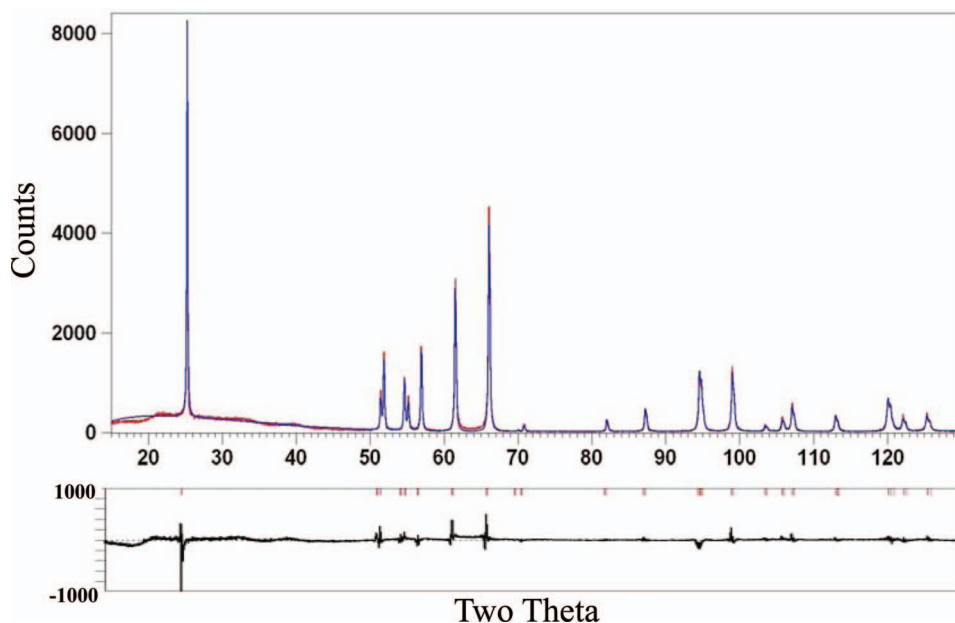


**Figure 1.** XRD pattern (red) and refinement (blue) of as-prepared NaNiO<sub>2</sub>. The broad peaks between 10° and 30° are due to the Kapton film. The red and blue lines represent the experimental and calculated data respectively. The residual discrepancy is shown in black. The refinement is performed in the C2/m space group and results in  $R_{wp} = 15.52\%$ , and  $\chi^2 = 4.06$ .

Galvanostatic measurements of charge and discharge of NaNiO<sub>2</sub> at C/10 at various cycles (1C = 235 mAh/g) and in two different voltage ranges (1.25–3.75 and 2.0–4.5 V) are shown in Figure 2. The charge and discharge curves show the expected step-like character.<sup>31,32</sup> Except for the first charge, the similarity in plateaus indicates that the charge and discharge processes go through the same phase transitions during the sodium extraction and insertion.

The charge/discharge capacities in the range of 1.25–3.75 V, Figure 2a, in the first, second, tenth and twentieth cycle are 147/123 mAh/g, 121/119 mAh/g, 119/118 mAh/g, and 117/116 mAh/g respectively. The coulombic efficiencies are 83.8% for the first cycle, 98.4% for the second cycle, 99.2% for the tenth cycle, and 99.2% for the twentieth cycle. When the same experiment is repeated in a higher voltage range (2–4.5 V, Figure 2b) the charge/discharge capacities in the first, second, tenth, and twentieth are 199/147 mAh/g, 136/128 mAh/g, 127/107 mAh/g, 113/98 mAh/g respectively. The coulombic efficiencies are 73.7% for the first cycle, 93.7% for the second cycle, 84.6% for the tenth cycle, and 86.3% for the twentieth cycle. There is clearly significant capacity decline when charging to high voltage, as well as a reduction in coulombic efficiency. The first charge is different from the subsequent charges, though above 3 V the profile is similar to the later charge curves indicating that some excess capacity is present at low voltage in the first charge.

Cyclic voltammetry (CV) data was collected to further investigate capacity decline as well as the difference between the charge and discharge profiles over cycling observed at higher voltage ranges, shown in Figure 3. The CV of NaNiO<sub>2</sub> (main plot) shows four series

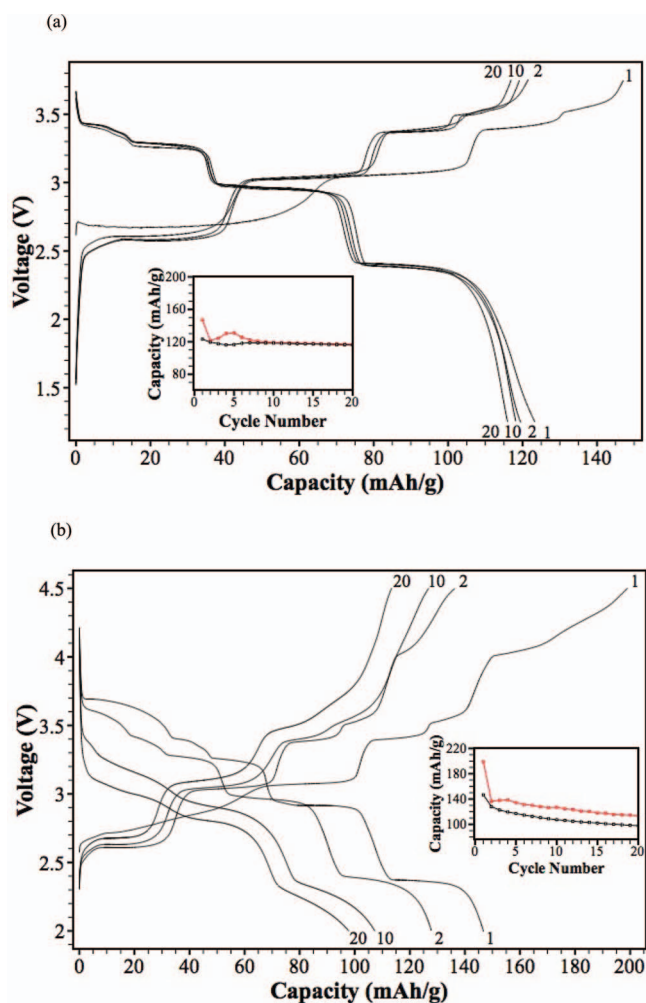


**Figure 2.** Voltage profile of NaNiO<sub>2</sub> after multiple cycles at C/10. The cell is galvanostatically cycled between a) 1.25–3.75 V b) 2.0–4.5 V.

**Table I.** Structural parameters of NaNiO<sub>2</sub>.

	unit cell parameters			occupancy	B isotropic
	x	y	z		
Ni	0.0	0.5	0.0	0.855	0.068
Na	0.0	0.0	0.5	1.000	2.527
O	0.2175(7)	0.0(0)	0.2032(7)	0.933	2.120
a = 5.3224(1), b = 2.84518(6), c = 5.5846(1), $\beta$ = 110.467(1), $R_{wp}$ = 15.52, $\chi^2$ = 4.06.					

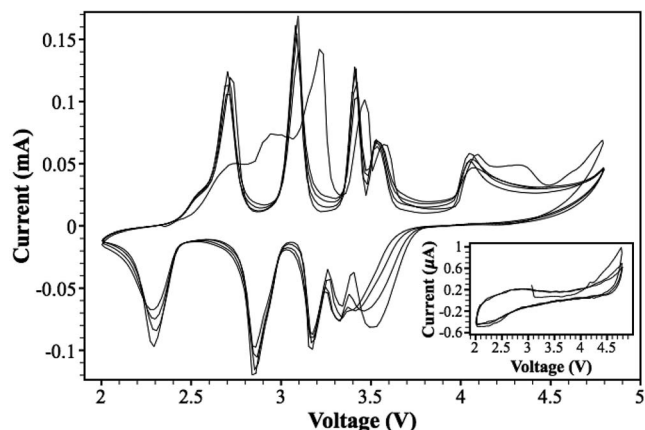


**Figure 3.** Comparison of the cyclic voltammetry (CV) data of  $\text{NaNiO}_2$  (main plot) and of the electrolyte (insert).

of reversible oxidation and reduction peaks at 2.7/2.3, 3.1/2.9, 3.4/3.2, 3.5/3.4 V. Except for the first cycle scan, the subsequent scans are very similar indicating good reversibility of the material in the 2.0–4.0 V domain. The oxidation peaks around 2.5 V–3.0 V in the first cycle are different from those of the consequential cycles, in agreement with the galvanostatic cycling where the first charge profile below 3.0 V is different from other cycles. The processes that occur upon charging above 4.0 V do not seem fully reversible as there are no corresponding reduction peaks near 4.0 V. These peaks may indicate side reactions that correlate to the poor cyclic performance when  $\text{NaNiO}_2$  is cycled at voltages higher than 4.0 V. The CV of the electrolyte on stainless steel electrodes vs. Na metal is shown as an insert. The current increases significantly above 4.0 V for the first cycle indicating the onset of oxidation of the electrolyte. After the first cycle the current levels are lowered indicating an effective passivation. This further indicates that after passivation stainless steel is a proper current collector.

Both galvanostatic and CV results show that reactions in the region between 2.5–3.0 V during the first charge are different from the following charges. XRD analysis was performed in order to investigate the changes in the material after the first cycle. Figure 4 compares the XRD of three samples. On the bottom of the figure (in black) is the XRD of the pristine  $\text{NaNiO}_2$  sample. The middle pattern (in red) is an XRD of the as-prepared electrode, when  $\text{NaNiO}_2$  has been mixed with PTFE and carbon black. Besides the pristine phase, a new phase is present, which can be matched with  $\text{Na}_{0.91}\text{NiO}_2$ . It is clear that a small amount of Na has been lost during the electrode preparation, either due to reactivity with air, or with the binder or carbon black material. The top graph (in blue) shows the XRD pattern of the discharges electrode after the first cycle between 2.0–3.75 V. The XRD pattern

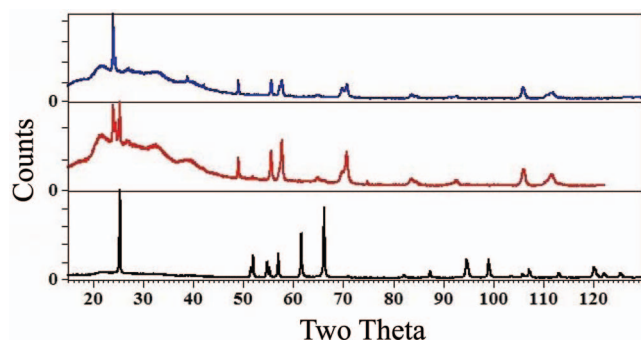


**Figure 4.** XRD pattern of  $\text{NaNiO}_2$  (black),  $\text{NaNiO}_2$  mixed with PTFE and carbon black (red), and cathode material after first cycle 2.0–3.75 V (blue). The broad peaks between  $10^\circ$  and  $30^\circ$  are due to the Kapton film.

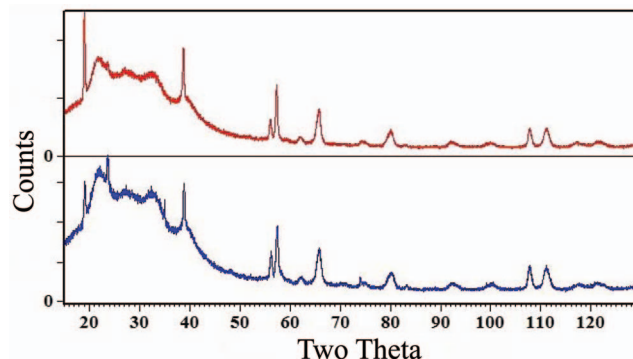


**Figure 5.** XRD pattern of the cathode that was charged to 3.75 V (red) and to 4.5 V (blue). The broad peaks between  $10^\circ$  and  $30^\circ$  are due to the Kapton film. The lattice parameters are  $a = 2.84$  and  $c = 20.8$ .

shows only the  $\text{Na}_{0.91}\text{NiO}_2$  phase without any  $\text{NaNiO}_2$  indicating that discharge does not proceed back to the fully sodiated  $\text{NaNiO}_2$ .

Further XRD analysis was done at higher voltage in order to investigate the reduction in capacity. The XRD patterns after charging  $\text{NaNiO}_2$  to 3.75 and 4.5 V, shown in Figure 5, are very similar, except for two additional peaks around  $23.7^\circ$  and  $35.0^\circ$  degrees present in the highly charged sample. These two additional peaks indicate the formation of a new phase, the structure of which we have not been able to identify.

Figure 6 shows the voltage profiles versus the composition of Na when the cells are cycled between 2.0–3.75 V and 2.2–4.5 V respectively with the potentiostatic intermittent titration technique (PITT). The voltage plateaus are similar to those obtained in galvanostatic mode, and while there is coulombic inefficiency the discharge profile appears similar in discharge and charge indicating a good degree of reversibility of the material. An apparent amount of 1.0 Na, corresponding to a charge capacity of 235 mAh/g, can be de-intercalated from  $\text{NaNiO}_2$  when the cell is charged up to 4.5 V vs.  $\text{Na}/\text{Na}^+$ . Upon discharge to 2.2 V, 0.62 Na, corresponding to a discharge capacity of 145 mAh/g, can be reversibly intercalated back. Hence, at this high charging voltage, some of the charging current does not seem to be related to Na extraction, but rather may involve oxidation reactions of the electrolyte. When  $\text{NaNiO}_2$  is charged to 3.85 V and discharged to 2.0 V, about 0.57 Na (135 mAh/g) and 0.46 Na (109 mAh/g) can be de-intercalated/intercalated respectively.

## Discussion

When  $\text{NaNiO}_2$  is cycled below 3.75 V, we observe a reversible voltage profile with  $\approx 120$  mAh/g reversible discharge capacity, which

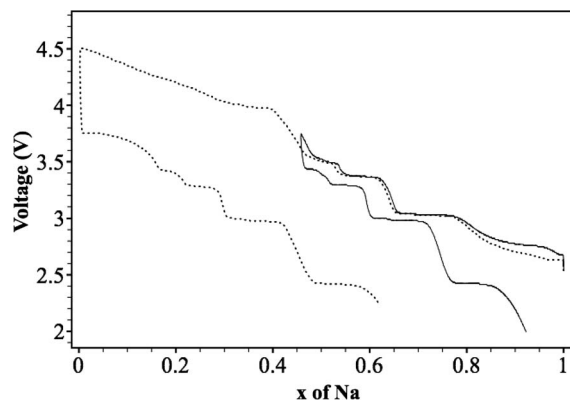


**Figure 6.** First cycle voltage profile of  $\text{Na}_x\text{NiO}_2$ . The cell is potentiostatically charged up to 4.5 (dashed) and 3.75 V (line) vs.  $\text{Na}/\text{Na}^+$  and discharged to 2.2 and 2.0 V respectively.



is a significantly improvement over previous reports which evaluated  $\text{NaNiO}_2$  with  $\text{NaClO}_4$  in PC as electrolyte and only demonstrated the de-intercalation of 0.2 Na per formula unit.<sup>5,30–33</sup> The reversibility of Na cycling in  $\text{Na}_x\text{NiO}_2$  is confirmed from the XRD analysis of the cathode after the first cycle (2.0–3.75 V), which shows that the material remains topotactically related to  $\text{NaNiO}_2$ , even though discharge proceeds back to  $\text{Na}_{0.91}\text{NiO}_2$ . At this point we do not understand why the  $\text{NaNiO}_2$  composition cannot be reached in discharge. Testing in two other electrolytes, 1 M  $\text{NaClO}_4$  in PC, and 1 M  $\text{NaBF}_4$  in EC:DMC showed similar initial capacities as with 1 M  $\text{NaPF}_6$  in EC:DMC but with somewhat higher capacity decay with cycling.

The voltage versus capacity shows very pronounced features with large voltage steps and plateaus as is expected for the step-like behavior of non-metallic bronzes.<sup>31,32</sup> The same plateaus are observed over 20 cycles indicating that the phase transitions with sodium de-intercalation/intercalation are highly reversible. Similar behavior with large voltage steps in the voltage curve has also been observed for de-intercalation of Na from  $\text{NaMnO}_2$ ,<sup>12</sup>  $\text{NaCoO}_2$ ,<sup>19,34</sup>  $\text{NaNi}_{0.5}\text{Mn}_{0.5}\text{O}_2$ <sup>19</sup> but it is a less common feature in Li-intercalation systems unless structural or electronic transitions are involved.<sup>35</sup>

It is not generally understood why voltage steps in Na intercalation compounds are so much more pronounced. In layered  $\text{Li}_x\text{MO}_2$  compounds plateaus and steps tend to be shorter and smaller and have been related to order-disorder transformations,<sup>36,37</sup> subtle stacking changes when all the alkali is removed,<sup>37</sup> or even to electronic transitions.<sup>35,38</sup> The magnitude of a step in the voltage curve is related to the energetic driving force with which the compounds at that concentration form, and the length of the plateau is related to the width of the two-phase region between compounds (in case of a first order transition).<sup>39</sup> To understand why the driving force for transition to intermediate  $\text{Na}_x\text{NiO}_2$  compounds is so much larger than for the  $\text{LiMO}_2$  materials will require a detailed characterization of these phases.

Pure Na-vacancy ordering, as often occurs with Li-vacancies<sup>37,40</sup> is possible, but the electrostatic interaction between  $\text{Na}^+$  ions is smaller than in the case of  $\text{Li}^+$  ions due to the larger lattice parameters of Na compounds. Due to its larger size strain effects will be much larger for  $\text{Na}^+$  and this can enhance ordering interactions. Stacking changes is another possibility: while  $\text{Li}_x\text{MO}_2$  compounds tend to remain in ABC oxygen stacking upon de-lithiation, except at a complete Li removal,<sup>41</sup> Na often prefers prismatic coordination by oxygen which can be achieved from the O3 structure by sliding the oxygen layers across the Na layer. If the stacking phase transitions take place, it is remarkable that they occur with high reversibility and with low voltage hysteresis. An alternative explanation, solely related to electronic structure changes has also been given.<sup>31,32</sup>

Both galvanostatic and CV test results show different voltage profile or oxidation peaks in the region 2.5–3.0 V during the first cycle in comparison with the following ones. In galvanostatic cycling, the 2.7 V plateau in the first charge is larger than in the subsequent charge cycles. This excess capacity may be due to several factors. Since the discharge only occurs to  $\text{Na}_{0.91}\text{NiO}_2$ , the second and subsequent charges start from a lower Na content. This accounts for most of the discrepancy between the first and subsequent charges. In addition, ICP shows extra Na content, which may be present as  $\text{Na}_2\text{O}$  or  $\text{Na}_2\text{CO}_3$  and show up in first charge.

When the cell is cycled between 2.0–4.5 V, the desodiation of  $\text{NaNiO}_2$  becomes irreversible, especially at higher voltage. An additional charge capacity of about 55 mAh/g appears between 3.75 V to 4.5 V in the first charge, but only an additional 30 mAh/g of this appears in discharge. In the following cycles, this additional capacity decays and disappears within 10 cycles. CV results confirm the irreversibility of the reactions above 4.0 V. Furthermore, PITT (Figure 6) gives an additional 100 mAh/g charge capacity between 3.85 V to 4.5 V but only ~30 mAh/g is recovered upon discharge, similar to what Komaba et. al. have observed with  $\text{NaNi}_{0.5}\text{Mn}_{0.5}\text{O}_2$ .<sup>19</sup> All the above electrochemical results suggest that some of the additional charge capacity between 3.75 V to 4.5 V is from electrolyte decomposition, which will not be shown in the discharge. The other part of the additional charge capacity that appears when charging to 4.5 V, which also

appears in the following discharge is likely from the further extraction of Na from the cathode, which leads to the formation of a new phase. The XRD of the charge samples seems to confirm this: The XRD patterns after charging  $\text{NaNiO}_2$  to 3.75 and 4.5 V are very similar except for the additional peaks around 23.7 and 35.0 degrees. These extra peaks indicate the formation of a new phase during overcharge. This phase formation seems to be largely irreversible as there is very little discharge capacity at the higher voltage. We speculate that this phase is formed as a passivating surface film. The formation of an inactive phase at the surface would also explain the increase polarization observed in the lower voltage region after charging to high voltage.

Ong, et. al. compared sodium-ion and lithium-ion intercalation materials and found that the Na voltages of the investigated compounds were 0.18–0.57 V lower than the corresponding Li voltages.<sup>42</sup> In this context it is instructive to compare  $\text{LiNiO}_2$  and  $\text{NaNiO}_2$ . The experimental average voltage of  $\text{LiNiO}_2$  is 3.85 V<sup>43</sup> in close agreement with the calculated voltage, 3.82 V.<sup>42</sup> Even though there is no experimental electrochemical data available for the complete voltage profile between  $\text{NaNiO}_2$  and  $\text{NiO}_2$  making a direct comparison to  $\text{LiNiO}_2$  not possible, when  $\text{NaNiO}_2$  is charged to 3.75 V the average voltage is 3.20 V. This value is close to the calculated voltage of 3.31 V.<sup>42</sup>

## Conclusions

Monoclinic  $\text{NaNiO}_2$  has been synthesized and tested electrochemically as a positive electrode material for a sodium ion battery. A series of well pronounced steps is observed in the voltage profile, which is very similar in charge and discharge. This indicates that  $\text{NaNiO}_2$  undergoes the same reaction path in the intercalation/de-intercalation process. In comparison to previous studies, we report that between 2.0–4.5 V, 0.85 Na can be de-intercalated and 0.62 Na intercalated back (corresponding to 199 mAh/g charge capacity and 147 mAh/g discharge capacity). Cycling at 1.25–3.75 V shows that 0.63 Na can be de-intercalated and 0.52 Na intercalated back reversibly (corresponding to 147 mAh/g charge capacity and 123 mAh/g discharge capacity). Upon cycling over 20 cycles, we observe that  $\text{NaNiO}_2$  has good stability when cycled in the lower voltage range, with no significant structural change and minor capacity fade.

## Acknowledgments

We thank the Samsung Advanced Institute of Technology for their funding of this research. This work made use of the Shared Experimental Facilities supported part by the MRSEC Program of the National Science Foundation under award number DMR-0819762.

## References

1. L. Zhang, K. Takada, N. Ohta, M. Osada, and T. Sasaki, *J. Power Sources*, **174**, 1007 (2007).
2. S. Komaba, C. Takei, T. Nakayama, A. Ogata, and N. Yabuuchi, *Electrochem. Comm.*, **12**, 355 (2010).
3. A. R. Armstrong and P. B. Bruce, *Nature*, **381**, 499 (1996).
4. C. Delmas, J. J. Braconnier, C. Fouassier, and P. Hagenmuller, *Solid State Ionics*, **3**, 165 (1981).
5. J. J. Braconnier, C. Delmas, and P. Hagenmuller, *Mat. Res. Bull.*, **17**, 993 (1982).
6. A. Maazaz, C. Delmas, and P. Hagenmuller, *J. Inclusion Phenom.*, **1**, 45 (1983).
7. S. Kikkawa, S. Miyazaki, and M. Koizumi, *J. Power Sources*, **14**, 231 (1985).
8. A. Mendiboure, C. Delmas, and P. Hagenmuller, *J. Solid State Chem.*, **57**, 323 (1985).
9. L. W. Shacklette, T. R. Jow, and L. Townsend, *J. Electrochem. Soc.*, **135**, 2669 (1988).
10. Y. Takeda, K. Nakahara, M. Nishijima, N. Imanishi, O. Yamamoto, M. Takano, and R. Kanno, *Mat. Res. Bull.*, **29**, 659 (1994).
11. C. Didier, M. Guignard, C. Denage, O. Szajwaj, S. Ito, I. Saadoune, J. Darriet, and C. Delmas, *Electrochem. Solid-State Lett.*, **14**, A75 (2011).
12. X. Ma, H. Chen, and G. Ceder, *J. Electrochem. Soc.*, **158**, A1307 (2011).
13. E. J. Wu, P. D. Tapesch, and G. Ceder, *Philos. Mag. B*, **77**, 1039 (1998).
14. T. A. Hewston and B. L. Chamberland, *J. Phys. Chem. Solids*, **48**, 97 (1987).
15. I. Saadoune, A. Maazaz, M. Menetrier, and C. Delmas, *J. Solid State Chem.*, **122**, 111 (1996).
16. J. M. Paulsen and J. R. Dahn, *Solid State Ionics*, **126**, 3 (1999).
17. Z. Lu and J. R. Dahn, *J. Electrochem. Soc.*, **148**, A1225 (2001).
18. M. M. Doeff, T. J. Richardson, and K. T. Hwang, *J. Power Sources*, **135**, 240 (2004).

19. S. Komaba, T. Nakayama, A. Ogata, T. Shimizu, C. Takei, S. Takada, A. Hokura, and I. Nakai, *ECS Trans.*, **16**, 43 (2009).
20. S. Komaba, N. Yabuuchi, T. Nakayama, A. Ogata, T. Ishikawa, and I. Nakai, *Inorg. Chem.*, **51**, 6211 (2012).
21. M. Sathiy, K. Hemalatha, K. Ramesha, J.-M. Tarascon, and A. S. Prakash, *Chem. Mat.*, **24**, 1846 (2012).
22. N. Yabuuchi, M. Kajiyama, J. Iwatate, H. Nishikawa, S. Hitomi, R. Okuyama, R. Usui, Y. Yamada, and S. Komaba, *Nat. Mat.*, **11**, 512 (2012).
23. D. Kim, E. Lee, M. Slater, W. Lu, S. Rood, and C. S. Johnston, *Electrochem. Comm.*, **18**, 66 (2012).
24. L. D. Dyer, B. S. Borie, and G. P. Smith, *J. Am. Chem. Soc.*, **76**, 1499 (1954).
25. S. Dick, M. Muller, F. Preissinger, and T. Zeiske, *Powder Diffr.*, **12**, 239 (1997).
26. E. Chappel, M. Nunez-Regueiro, G. Chouteau, O. Isnard, and C. Darie, *Eur. Phys. J. B*, **17**, 615 (2000).
27. M. Sofin and M. Jansen, *Z. Naturforsch.*, **60b**, 701 (2005).
28. J. P. Parant, R. Olazcuaga, M. Devalette, C. Fouassier, and P. Hagenmuller, *J. Solid. State. Chem.*, **3**, 1 (1997).
29. M. Jansen and R. Hoppe, *Z. Anorg. Allg. Chem.*, **399**, 163 (1973).
30. S. Miyazaki, S. Kikkawa, and M. Koizumi, *Synth. Met.*, **6**, 211 (1983).
31. J. Molenda and A. Stoklosa, *Solid State Ionics*, **38**, 1 (1990).
32. J. Molenda, *Solid State Ionics*, **21**, 263 (1986).
33. C. Delmas, J. J. Braconnier, A. Maazaz, and P. Hagenmuller, *Rev. Chim. Miner.*, **19**, 343 (1982).
34. R. Berthelot, D. Carlier, and C. Delmas, *Nat. Mat.*, **10**, 74 (2011).
35. M. Menetrier, I. Saadoune, S. Levasseur, and C. Delmas, *J. Mater. Chem.*, **9**, 1135 (1999).
36. J. N. Reimers and J. R. Dahn, *J. Electrochem. Soc.*, **139**, 2091 (1992).
37. A. Van der Ven, M. K. Aydinol, G. Ceder, G. Kresse, and J. Hafner, *Phys. Rev. B*, **58**, 2975 (1998).
38. C. A. Marianetti, G. Kotliar, and G. Ceder, *Nat. Mat.*, **3**, 627 (2004).
39. G. Ceder and A. Van der Ven, *Electrochem. Acta*, **45**, 131 (1999).
40. H. W. Zandbergen, M. Foo, Q. Xu, V. Kumar, and R. J. Cava, *Phys. Rev. B*, **70**, 024101 (2004).
41. G. G. Amatucci, J. M. Tarascon, and L. C. Klein, *J. Electrochem. Soc.*, **143**, 1114 (1996).
42. S. P. Ong, V. L. Chevrier, G. Hautier, A. Jain, C. Moore, S. Kim, X. Ma, and G. Ceder, *Energy Environ. Sci.*, **4**, 3680 (2011).
43. C. Delmas, M. Menetrier, L. Croguennec, S. Lavasseur, J. Peres, C. Pouillier, G. Prado, L. Fournes, and F. Weill, *Int. J. Inorg. Mater.*, **1**, 11 (1999).